Int. J. Rock Mech. Min. Sci. & Geomech. Abstr. Vol. 30, No. 7, pp. 965–971, 1993
Printed in Great Britain

0148-9062/93 $6.00 + 0.00
Pergamon Press Ltd

Near-surface, "Thin Skin" Reverse Faulting Stresses in the Southeastern United States

DANIEL MOOS†
MARK D. ZOBACK†

Hydraulic fracturing stress measurements have been conducted in crystalline rock at two locations within the southeastern United States at depths from 50 meters to more than one kilometer. Stress orientations are similar to those obtained from other local and regional stress indicators and are consistent with a ridge-push source of intraplate stress. 'High horizontal stress magnitudes (with respect to the vertical stress) are found only in the near-surface.' Thus, although relatively shallow stress orientation measurements appear to be reliable indicators of the stress orientation at greater depth, stress magnitudes cannot be extrapolated quantitatively beyond the depth range of the measurements.

INTRODUCTION

One approach to the assessment of earthquake hazards to structures is to determine the capability of mapped or inferred faults through analysis of the magnitudes and orientations of the in situ principal stresses. Furthermore, knowledge of the in situ stress state is interesting in itself because of the insights such knowledge can provide on the forces driving the earth's plates. Data on the present-day stress orientation can be provided by a number of indirect techniques (see Zoback et al. [1] for a review). Fortunately, it has been found that the orientations of in situ stresses at shallow depth are generally quite similar to those inferred from earthquake focal mechanisms at substantially greater depths [2]. However, it is less clear whether stress magnitudes at depth can be extrapolated from shallower measurements. This paper presents the results of in situ stress measurements carried out in two locations in the southeastern United States. In these instances, the orientations of the horizontal principal stresses within the uppermost few hundred meters are similar to those at greater depth inferred from earthquake focal plane mechanisms, but the relative stress magnitudes are quite different.

SITE LOCATIONS AND EXPERIMENTAL TECHNIQUE

Figure 1 shows the locations of the study areas. The first site study was carried out within basement rocks of the Inner Piedmont (Hole 1), the Chauga Belt, including the Brevard Fault Zone (Hole 2), and the Blue Ridge (Hole 4) in the Appalachian Deep Core Hole (ADCOH) Site Survey Area. Hydraulic fracturing, borehole televiewer (BHTV) and other geophysical logging experiments were carried out to depths of 304.8 m (Holes 1 and 2), and 414.5 m (Hole 4). In all three cases, basement rocks extended to within less than 20 meters of the surface.

The second study area was within the Savannah River Site (SRS). Basement rocks were overlain in this area by about 300 meters of sediments. A complete set of experiments were carried out in Holes SSW-1, SSW-2, DRB-8, and NPR-1, drilled into Paleozoic and pre-Cambrian age metamorphic rock of the Charlotte and slate belt groups, and BHTV logs were recorded in DRB-11, drilled into Triassic-age sands and mudstones within the NE-SW trending Dunbarton Basin which underlies much of the site.

Results of a similar set of measurements, carried out at the Monticello Reservoir, South Carolina will also be discussed briefly (see [3, 4] for further details).

The experimental procedure in all cases was similar. Geophysical logs were recorded to study the in situ variation in physical properties, a borehole televiewer survey was run to map the orientation and distribution of

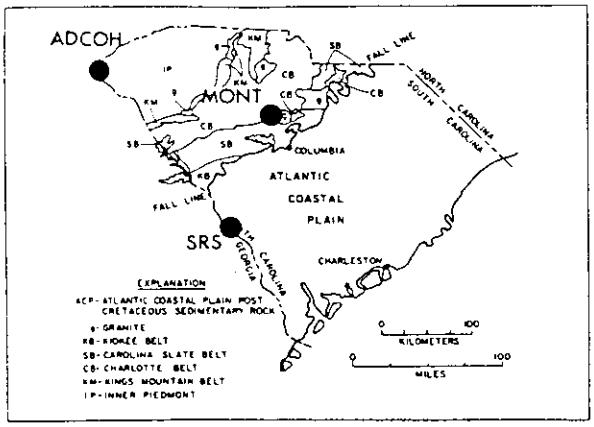

Fig. 1. Geologic map of South Carolina, showing the locations of the sites at which hydraulic fracturing stress measurements were made.

†Department of Geophysics, Stanford University, Stanford, CA 94305-2215

pre-existing (natural) fractures and foliation planes, to determine the cross-sectional shape of the wellbore, and to find evidence of wellbore failure (breakouts). Intervals for hydraulic fracturing tests were selected on the basis of the televiewer logs and, where possible, from examination of the recovered core. Criteria for choosing intervals for testing are that the hole is cylindrical and that the interval contains no pre-existing fractures.

Hydraulic fracturing experiments were then carried out within the selected intervals, following techniques similar to those described by Hickman and Zoback [5]. In these experiments pressures and flow rates were measured at the surface and recorded digitally for graphical analysis. We verified the assumption that downhole pressures could be determined simply by adding the static head to the surface pressure measurements, by comparing pressures recorded at the test interval in a number of tests using a mechanical transducer. Data were analyzed using techniques discussed by Hickman and Zoback [5] and Baumgärtner and Zoback [6].

Least principal stress magnitudes were determined from shut in pressures in a variety of ways, including using the crack tip closure pressure [7], which was found to give excellent results for the studies conducted at SRS. As in general both horizontal stresses were greater than the vertical stress, early-cycle shut-in pressures were used to determine S_{hmin}, and in some cases late-stage shut-in pressures indicated that the fractures rotated into the horizontal plane, providing a measure of S_v. Greatest principal stresses were determined from fracture reopening pressures, based on the standard assumption that the borehole is drilled in the direction of the vertical stress which is itself a principal stress, and that the rock behaves elastically so that the concentration of stress around the wellbore can be expressed using the 2-D Kirsch equations [8], as modified by Bredehoeft et al. [9]. As there is also considerable discussion about the importance of pore pressure in fracture reopening [10, 11], the maximum horizontal compressive stress was computed both with and without pore pressure, to provide upper and lower bounds on S_{Hmax}:

$$3S_{hmin} - P_{b(T=0)} - P_p \le S_{Hmax} \le 3S_{hmin} - P_{b(T=0)} \quad (1)$$

In order to evaluate the likelihood of earthquakes, the stress magnitudes determined from the hydraulic fracturing measurements are compared to the stress magnitudes required to cause slip on cohesionless, well-oriented faults with coefficients of friction between 0.6 and 1.0 (within the range of laboratory measurements [12]). These limits are computed from the assumption that a well-oriented fault will slip if the ratio of the effective maximum and minimum stresses exceeds its frictional strength:

$$(S_1 - P_p)/(S_3 - P_p) = ((1+\mu)^{1/2} + \mu)^2 \quad (2)$$

Hydraulic fracture orientations were determined either using a magnetically-oriented impression packer [13] or by analysis of a second borehole televiewer log recorded after hydraulic fracturing. In the case of the ADCOH holes, fractures were located using the BHTV; both oriented impressions and BHTV images were used to locate fractures at the SRS. Most of the fractures were found to be axial, although in some cases it appeared that the fractures were created in the plane of the generally steeply-dipping foliation.

STRESS RESULTS

ADCOH Site Survey Holes

Good quality stress magnitude information was obtained from each of the three coreholes. The measured values of P_b and ISIP, as well as the calculated S_{hmin}, S_{Hmax}, T and P_p values are presented in Table I. The uncertainty in the value of S_{hmin} simply represents the accuracy to which the shut-in pressure can be measured using the pressure/time curves. The range of S_{Hmax} values is a consequence of both the uncertainty in picking the pressures and the result of including (lower bound) or ignoring (upper bound) the pore pressure in Eqn. 1. Figure 2 summarizes the data obtained in the three Site Survey coreholes.

In all cases, the magnitudes of both horizontal stresses exceed the calculated lithostat. The maximum horizontal stress follows the limit for frictional equilibrium for μ=0.6 in Hole 1. In Hole 2 (which penetrated the Brevard Fault Zone) S_{Hmax} is only slightly greater than the lithostat below 100 meters. However, in Hole 4, which penetrated Blue Ridge metamorphic rocks, stresses are above the value necessary to cause reverse faulting for μ=0.6 throughout the total depth of the hole. Stresses increase smoothly with depth only in Hole 1, which BHTV and geophysical logging revealed to contain few zones of intensely fractured, low velocity/resistivity rock [14]. In Holes 2 and 4, which contained several such zones, they are associated with stepwise changes in stress magnitude. For example, a stepwise increase in stress is seen across a breccia zone at approximately 235 m depth in Hole 4. And, in Hole 2, stresses similarly increase abruptly across fractured zones at 75 and 160 meters.

The aggregate orientation of hydraulic fractures imaged with the borehole televiewer was N50°E [14]. This implies a NE orientation of S_{Hmax}, consistent with other stress indicators within the region [2].

Savannah River Site

Figure 3 and Table II present the results of the hydraulic fracturing tests in Holes SSW-1, SSW-2, DRB-8, and NPR-1. Both horizontal principal stresses exceed the vertical stress at shallow depth. In general stresses are highest in DRB-8 and in NPR-1, and lowest in SSW-2. In DRB-8 and NPR-1, a number of hydraulic fractures appear to have turned into horizontal planes, and several tests seem to have initiated a horizontal fracture at the well bore. All of these data indicate that the vertical stress is nearly identical to that expected from the weight of the overburden.

The horizontal stresses increase quite slowly with depth, as illustrated by the results from the NPR-1 hole, and below a depth of about 800 meters the least principal stress is horizontal. Taking the average value of S_{hmin}

Table I - Hydraulic fracturing results in the ADCOH Site Survey coreholes

Depth (m)	P_b (MPa)	ISIP (MPa)	P_b(T=0) (MPa)	T (MPa)	P_p[1] (MPa)	S_v[2] (MPa)	S_{hmin} (MPa)	S_{Hmax} (MPa)
ADCOH 1								
81.8	19.3	3.8±.2	6.9	12.5	0.8	2.2	3.8	3.9-4.7
144.8	22.1	6.6±1	9.8	12.3	1.4	3.8	6.6	8.6-10.1
210.9	13.1	7.3±.3	7.8	5.3	2.1	5.6	7.3	11.8-14.0
281.6	27.5	10.2	11.8	15.7	2.8	7.5	10.2	15.8-18.7
ADCOH 2								
71.6	15.2	2.8±.4	5.4	9.82	0.7	1.9	2.8	2.3-3.0
95.7	17.7	5.0±.9	6.5	11.2	1.0	2.5	5.0	7.5-8.5
162.2	9.8	3.6±.2	5.8	4.0	1.6	4.3	3.6	3.2-4.8
193.2	16.8	7.0±.9	9.6	7.3	1.9	5.1	7.0	9.4-11.4
237.4	13.8	6.9±.6	8.7	5.2	2.4	6.3	6.9	9.6-12.0
277.0	16.7	8.2±.1	9.5	7.1	2.8	7.3	8.2	12.3-15.2
ADCOH 4								
82.3	18.4	4.2±.6	8.1	10.3	0.8	2.2	4.2	3.8-4.6
132.6	17.7	6.9±.9	8.1	9.6	1.3	3.5	6.9	11.2-12.6
169.2	16.6	7.1±.2	7.7	8.9	1.7	4.5	7.1	11.9-13.0
178.9	16.4	8.1±.5	7.6	8.8	1.8	4.7	8.1	14.9-16.7
215.5	23.0	9.1±1.1	9.9	13.1	2.1	5.7	9.1	15.1-17.3
265.8	41.7	15.9±.5	22.5	19.1	2.7	7.0	15.9	22.6-25.3
340.1	41.8	18.0±1.4	23.7	18.1	3.4	9.0	18.0	27.0-30.4

1) Calculated using the observed depth to the water table

2) Calculated assuming an average density of 2.65 gm/cm^3

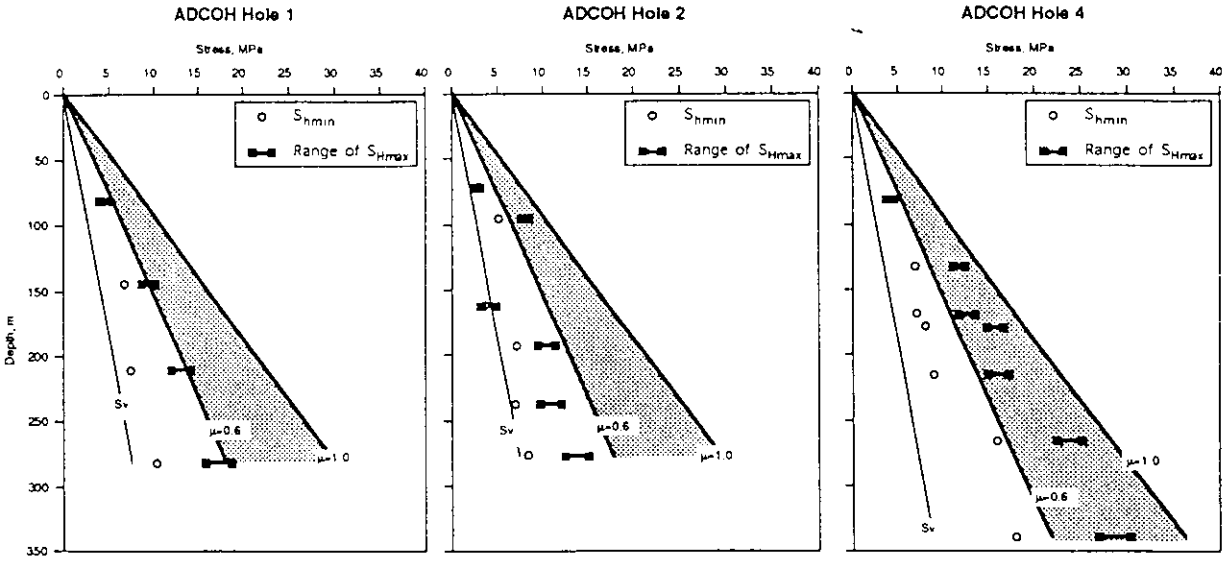

Fig. 2. Stress magnitudes in the ADCOH Site Survey boreholes. S_v is assumed to be equal to the weight of overlying rock, calculated using a density of 2.65 gm/cm^3. Also shown are the magnitudes of the maximum horizontal stress which would cause slip along well-oriented reverse faults for coefficients of sliding friction μ=0.6 and 1.0.

for the two measurements near 1050 meters, the magnitude of S_{Hmax} is only slightly less than that required to generate slip on well-oriented strike-slip faults. It is clear that if we attempt to linearly extrapolate the stress magnitudes we measure above 1 km to greater depth we encounter serious problems at depths of only a few km, as the extrapolated maximum horizontal stress drops below the vertical stress, which implies an extensional state of stress in the midcrust within a region that is generally characterized by horizontal compression.

Orientations of the hydraulic fractures were determined both by post-fracturing borehole televiewer logging and by running magnetically oriented impression packers (Table II). All but one fracture was found in the NE quadrant. The orientations of the hydraulicallly induced fractures suggest a roughly N65^{o}E direction of S_{Hmax}, consistent with other regional stress indicators [2].

Table II - Hydraulic fracturing results in the SRS boreholes

Depth (m)	P_b (MPa)	ISIP (MPa)	P_b(T=0) (MPa)	T (MPa)	P_p[1] (MPa)	S_v[2] (MPa)	S_{hmin} (MPa)	S_{Hmax} (MPa)	S_v[3] (MPa)	Orientation[4]	Quality	Comments
SSW-1												
329	21.2	11.1±.2	12.8±.8	8.4±.8	2.9	6.6	11.1±.2	17.1-19.9	--	N89°E(IP)	G	near vertical fracture
347	20.2	11.0±.4	15.8±.7	4.4±.7	3.0	7.0	11.0±.4	12.3-16.1	--			
353	22.8	12.7±.3	17.3±1.2	5.5±1.2	3.0	7.2	12.7±.3	15.7-19.9	--			
391	25.2	14.6±.4	21.7±1.0	3.5±1.0	3.4	8.2	14.6±.4	16.5-20.9	--	N64°E(IP)	E	vertical fracture
392.5	21.3	15.0±.6	15.5±1.0	5.8±1.0	3.4	8.3	15.0±.6	23.3-28.9	--	N61°E(IP)	E	vertical fracture
394	21.9	14.6±.3	15.7±.8	6.2±.8	3.4	8.3	14.6±.3	23.0-26.4	--			
418	21.9	14.7±.2	15.4±1.6	6.5±1.6	3.7	9.0	14.7±.2	22.8-27.2	--	N30°-50°±20°(B)	P	near vertical fracture
SSW-2												
303	16.1	11.0±.4	12.4±1.0	3.7±1.0	3.0	6.0	11.0±.4	15.4-19.8	--	S69°E(IP)[5]	E	vertical fracture
338	18.7	10.3±.4	14.9±.5	3.8±.5	3.3	7.0	10.3±.4	11.0-14.4	--			
360	25.4	10.5±.1	14.2±.8	11.2±.8	3.5	7.6	10.5±.1	12.7-14.9	--	N62°E	F	34° East dip-foliation plane
379	19.3	11.7±.4	13.1±1.0	6.0±1.0	3.7	8.2	11.7±.4	16.1-20.5	--			
386	20.8	12.0±.1	14.8±.8	6.0±.8	3.8	8.6	12.0±.1	16.3-18.5	--			
DRB-8												
352	24.7	15.4±.5	17.6±1.6	9.1±1.6	3.2	8.0	15.4±.5	22.3-28.5	8.7			fracture rolled over
363	22.6	18.6±.4	19.6±1.4	3.0±1.4	3.3	8.4	18.6±.5	30.0-35.8	--	N66°E(IP)	E	vertical fracture
396	25.7	16.1±.5	17.0±.3	8.7±.3	3.6	9.2	16.1±.5	25.9-29.5	8.6±1.0	N45°E(IP)	F	60° dipping frac, rolled over
404	15.9	--	8.0±.3	7.9±.3	3.7	9.4	--	--	6.7?			possible packer failure
412	18.0	--	10.3±.5	7.7±.5	3.8	9.6	--	--	9.8			probable horizontal fracture
426	18.0	--	11.4±.6	6.6±.6	3.9	10.0	--	--	6.5?			possible packer failure
434	32.3	--	8.2±.1	24.1±.1	4.0	10.2	--	--	6.2?			possible packer failure
453	39.9	--	8.8±.5	31.1±.5	4.2	10.8	--	--	7.6±.2?			possible packer failure
493	23.5	--	12.1±.5	11.4±.5	4.6	11.9	--	--	9.9			possible packer failure
501	34.2	21.7±.3	26.5±1.2	7.7±1.2	4.6	12.1	21.7±.3	31.9-36.1	--			
542	44.2	19.5±.5	35.6±1.0	8.6±1.0	5.0	13.2	19.5+.5	--	--			intersected sub-horizontal plane lower bound on S_{hmin} only
NPR-1												
378	27.9	14.8-16.0	19.1	8.8	3.5	7.8	14.8-16.0	21.8-28.9	—	N75°E, vert (B)		tensile strength moderate
468	35.3	8.7	9.3	26.0	4.5	10.5	—	—	8.7	horiz., (B)		created horizontal
560	41.4	10.3	10.5	30.9	5.4	13.2	—	—	10.3	horiz., (B)		created horizontal
590	36.5	23.6-23.8	29.0-31.0	5.5-7.5	5.7	14.1	23.6-23.8	34.1-42.4				low tensile strength
637	35.3	18.8-19.0	15.0-15.6	19.7-20.3	6.2	15.7	18.8-19.0	34.6-42.0	13.7-13.9			rotated to horizontal
733	32.7	19.3-19.9	20.6-22.2	10.5-12.1	7.2	18.7	19.3-19.9	28.5-39.1	16.0-16.6	N58°E, incl. (IP)		rotated to horizontal
1037	33.9	19.6-20.6	21.8-23.0	10.9-12.1	10.2	27.8	19.6-20.6	25.5-40.0	—	prob. vert. (IP)		not oriented
1039	35.5	23.5-23.9	25.5-26.5	7.5-10.0	10.3	27.9	23.5-23.9	33.7-46.2	—	prob. vert. (IP)		not oriented

(1) calculated using the observed depth to the water table

(2) calculated assuming 1.95 gm/cm^3 for sediments and 2.8 gm/cm^3 for basement rock (SSW-1; SSW-2; DRB-8) or by integrating a density log in basement (NPR)

(3) measured from instantaneous shut-in after pumping a large volume of fluid, assumes that the fracture "rolled over" into a horizontal plane

(4) with respect to True North determined from oriented impression packer (IP) or post-fracturing BHTV logging (BHTV)

(5) orientation incorrect possibly due to a stuck compass

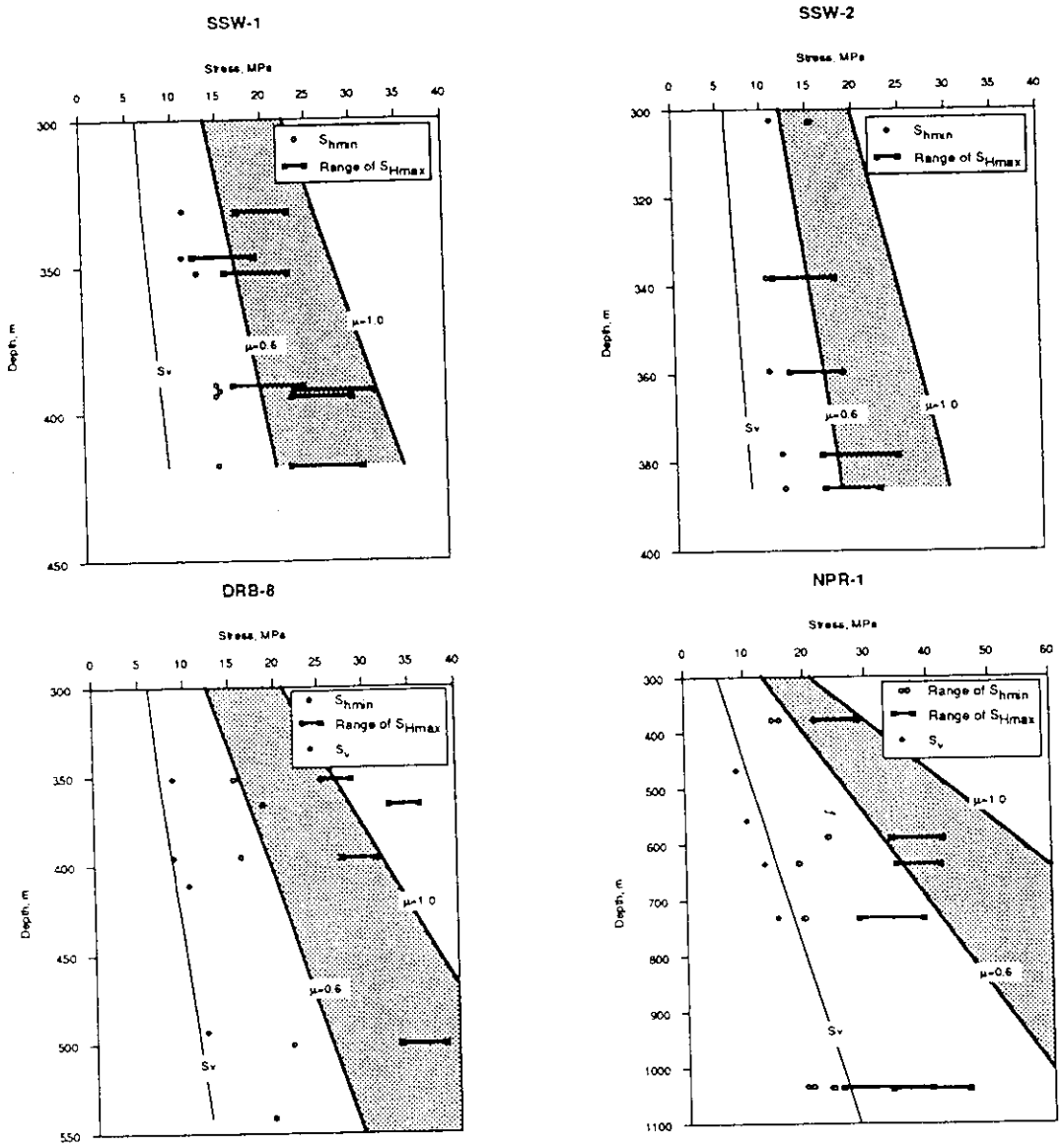

Fig. 3. Stresses calculated from hydraulic fracturing tests conducted within SSW-1, SSW-2, DRB-8 and NPR-1, along with the vertical stress calculated by integrating a density log (NPR-1) or from an assumed density in the sediments of 1.9 and in basement of 2.8 gm/cm^3 (for the other holes). Lines showing the upper bound on the horizontal stresses for reverse faulting on planes with coefficients of sliding friction μ=0.6 and 1.0 are also shown.

Wellbore breakouts, defined as sections within which a wellbore is elongated due to compressive shear failure of the rock at the azimuth of S_{hmin} [15, 16], were detected between 380 and 405 meters in DRB-11, and below about 600 meters in NPR-1. Figure 4a presents a histogram of maximum horizontal stress orientations determined from the breakouts in DRB-11. As shown in the figure, the direction of maximum principal horizontal stress determined from breakouts within the Triassic rock penetrated by DRB-11 is N55°-70°E. In contrast, the orientations of breakouts detected in the NPR hole suggest a maximum horizontal compression direction of N33°E (Fig. 4b). This is about 20-30° more northerly than that found at shallow depth both from hydraulic fracture orientations in SSW-1, SSW-2, and DRB-8 and from the breakouts in DRB-11.

To investigate the cause of this difference, we plot the midpoints of the breakouts as a function of depth in the NPR hole in Figure 4c. Although it is clear that they have a generally consistent NW-SE orientation, the breakouts between 900 and slightly less than 1200 meters are rotated about 20-30 degrees counterclockwise compared to those at shallower and at greater depths As most of the breakouts are within this apparently anomalous region, the histogram shows a corresponding orientation shift between these data and those from shallower depth in DRB-11.

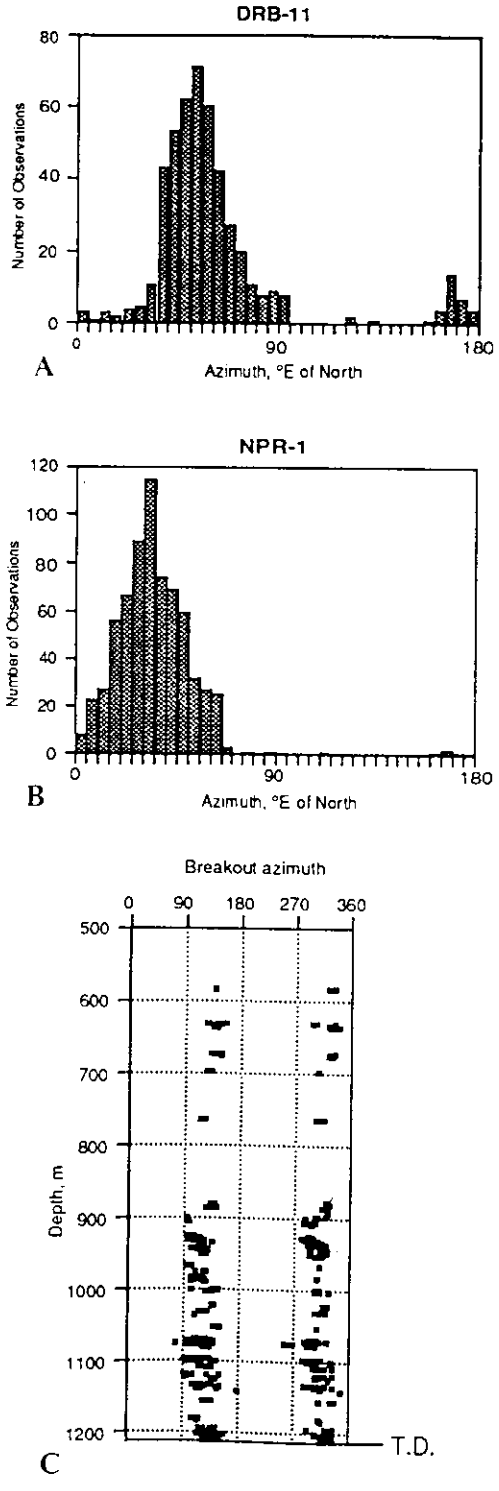

Fig. 4. A.) Histogram of the maximum horizontal principal stress orientations from breakouts in DRB-11, which yield an average orientation of N55-70°E for S_{Hmax}. B.) Histogram of S_{Hmax} directions inferred from the breakout data in NPR-1. The average azimuth of S_{Hmax} predicted from these measurements is N33°E (±15°). C.) Breakouts plotted as a function of depth within NPR-1. Although the shallowest breakouts suggest a roughly N60°E S_{Hmax} orientation, the breakouts can be seen to rotate slightly counterclockwise at intermediate depths, yielding an aggregate more northerly orientation of S_{Hmax}. Near the bottom of the hole the breakout orientation is again similar to that found at shallow depth in this hole and within the Triassic rocks penetrated by DRB-11.

DISCUSSION

The region of the southeastern United States within which these measurements were made is characterized by a fairly consistent NE-SW direction of maximum horizontal compressive stress, defined by focal mechanisms of recent earthquakes, young geologic indicators, and direct measurements of in situ stress [2]. Furthermore, the aggregate orientations of S_{Hmax} from shallow data and from deeper earthquake focal mechanisms are the same (about N70°E). Shallow seismicity in the region, particularly within crystalline terranes, is predominantly reverse in character [17].

The measured stress magnitudes at the SRS and in the ADCOH Site Survey region suggest a highly compressional near-surface stress field that is capable of causing reverse faulting on well-oriented pre-existing planes of weakness. Similar results were found at the Monticello Reservoir [3, 4] (for location see Fig. 1), and at Kent Cliffs, New York [18] and Moodus, Connecticut [19, 20]. McGarr and Gay [21] and Brace and Kohlstedt [22] summarize numerous results from Canada and S. Africa of very high horizontal stresses in the uppermost few hundred meters of cratonic crust, even though in the case of S. Africa the tectonic stresses at greater depth favor normal faulting. Similar stresses have been observed in Fennoscandia [23].

Voight and St. Pierre [24] proposed that high horizontal stresses in crystalline rocks in the near-surface could result from denudation, although McGarr and Gay [21] dispute this. It is more likely that high stresses at shallow depth are simply an expression of the response of the lithosphere to the forces driving the plates. In other words, compressional regional tectonic forces are distributed in such a way that there is an excess horizontal stress at shallow depth in regions in which strong, elastic rock extends to the surface. This leads to very high near-surface ratios of horizontal to vertical stress, as S_V approaches zero at shallow depth. Where weaker rocks overly mid crustal materials, they deform more readily and may consequently exhibit a lower level of horizontal stress. For example, stress magnitudes measured in Coastal Plain sediments near Charleston, S.C. were quite low [25]. However, the orientation of the maximum horizontal stress is generally aligned with the regional tectonic force.

Perhaps the most important question related to seismic risk is whether high stresses measured at shallow depth (and the accompanying low-magnitude seismicity)

can be related to the possibility of potentially damaging earthquakes at greater depths. In general, this appears unlikely. For example, at Monticello the deepest earthquakes are limited to about 2.5 km [17]. In this and other cases the shallow seismicity may be totally unrelated to the potential for deeper earthquakes. In cases where high horizontal stresses are suspected to be present at greater depth, careful monitoring of earthquake hypocentral depths and deeper stress measurements are required to determine the depth to which the highly compressive stress field persists.

CONCLUSIONS

Hydraulic fracturing stress measurements and wellbore breakouts detected by borehole televiewer logging at two locations within the southeastern United States reveal a consistent, NE-SW orientation of S_{Hmax}. Although the S_{Hmax} orientation varies somewhat as a function of depth, possibly as a result of local geological complexity, it is the same at shallow depth as at much greater depth, and is generally consistent with a ridge-push source of intra-plate stress. High horizontal stresses detected at shallow depth, sometimes associated with small magnitude local seismicity, do not persist to greater depth. In fact, the near-surface reverse faulting stress field apparently does not extend below the uppermost few hundred meters of crystalline basement. This "thin skin" reverse faulting environment is most likely a consequence of the distribution of plate driving stresses in regions in which strong, elastic rock extends to the surface.

REFERENCES

1. Zoback, M. L., et al., Global patterns of tectonic stress, *Nature*, 341, 291-298 (1989).
2. Zoback, M. D. and Zoback, M. L., Tectonic stress field of North America and relative plate motions in *Neotectonics of North America* vol. 1, D. B. Slemmons, E. R. Engdahl, M. D. Zoback, D. D. Blackwell, Eds., Geological Society of America, Decade Map, Boulder, CO, 339-366, (1991).
3. Zoback, M. D. and Hickman, S., In situ study of the physical mechanisms controlling induced seismicity at Monticello reservoir, South Carolina, *J. Geophys. Res.*, 87, 6959-6974 (1982).
4. Haimson, B. C. and Lee, M. Y., Development of a wireline hydrofracturing technique and its use at a site of induced seismicity, 25th Symposium on Rock Mechanics (ROCK MECHANICS ON PROTECTION AND PRODUCTIVITY), Society of Mining Engineers of AIME, New York, N.Y., (1984).
5. Hickman, S. H. and Zoback, M. D., The interpretation of hydraulic fracturing pressure-time data for in situ stress determination, Workshop on Hydraulic Stress Measurements, U.S. National Committee on Rock Mechanics, Washington, D.C., 1-11, (1983).
6. Baumgärtner, J. and Zoback, M. D., Interpretation of hydraulic fracturing pressure - time records using interactive analysis methods, *International Journal of Rock Mechanics and Mining Sciences & Geomechanical Abstracts*, 26, 461-469 (1989).
7. Hayashi, K. and Sakurai, I., Determination of instantaneous shut-in pressures in hydraulic fracturing tectonic stress measurements, Proc. Int. HDR Geothermal Energy Conference, Cornwall, 27-30 June, (1989).
8. Hubbert, M. K. and Willis, D. G., Mechanics of hydraulic fracturing, *J. Petrol. Tech.*, 9, 153-168 (1957).
9. Bredehoeft, J. D., Wolff, R. G., Keys, W. S. and Shuter, E., Hydraulic fracturing to determine the regional in situ stress field, Piceance Basin, Colorado, *Geological Society of America Bulletin*, 87, 250-258 (1976).
10. Schmitt, D. R. and Zoback, M. D., Laboratory test of the effects of pore pressure on tensile failure, V. Maury, D. Fourmaintraux, Eds., Rock at Great Depth, Proceedings ISRM-SPE International Symposium, A.A.Balkema, Elf Aquitaine, Pau, (1989).
11. Zoback, M. D. and Healy, J. H., In situ stress measurements to 3.5 km depth in the Cajon Pass scientific research borehole: Implications for the mechanics of crustal faulting, *Journal of Geophysical Research*, 97, 5039-5057 (1992).
12. Byerlee, J. D., Friction of rock, *Pure Appl. Geophys.*, 116, 615-626 (1978).
13. Anderson, T. O. and Stahl, E. J., A study of induced fracturing using an instrumental approach, *Soc. Petrol. Eng. Jour.*, , 261-267 (1967).
14. Coyle, B. J., Zoback, M. D. and Moos, D., In-situ stress and fracture studies in three ADCOH site survey core holes (abs.), *EOS, Trans. AGU*, 67, 1242 (1986).
15. Bell, J. S. and Gough, D. I., The use of borehole breakouts in the study of crustal stress in *Hydraulic Fracturing Stress Measurements* M. D. Zoback, B. C. Haimson, Eds., National Academy Press, Washington, D.C., 201-209, (1983).
16. Zoback, M. D., Moos, D., Mastin, L. and Anderson, R. N., Wellbore breakouts and in situ stress, *J. Geophys. Res.*, 90, 5523-5530 (1985).
17. Talwani, P., Rastogi, B. K. and Stevenson, D., Tenth Tech. Report to the U.S. Geological Survey, contract #14-08-0001-17670, Induced seismicity and earthquake prediction studies in South Carolina (1980).
18. Zoback, M. D., Anderson, R. N. and Moos, D., In situ measurements in a 1 km-deep well near the Ramapo fault zone (abs.), *EOS, Trans. AGU*, 66, 363 (1985).
19. Zoback, M. D., Baumgärtner, J. and Moos, D., Hydraulic fracturing stress measurements in the Moodus Research Borehole and shallow earthquakes, (abs), *EOS, Trans. AGU*, 69, 491-492 (1988).
20. Moos, D., Zoback, M. D., Paillet, F. and Barton, C., Stress orientation and magnitude from wellbore breakouts in the Moodus Research Borehole -- comparison with regional data, (abs), *EOS, Trans. AGU*, 69, 492 (1988).
21. McGarr, A. and Gay, N. C., State of stress in the earth's crust, *Ann. Rev. Earth Planet Science*, 6, 405-436 (1978).
22. Brace, W. F. and Kohlstedt, D. L., Limits on lithospheric stress imposed by laboratory experiments, *Journal of Geophysical Research*, 85, 6248-6252 (1980).
23. Stephannson, O. and Angman, p., Hydraulic fracturing stress measurements at Forsmark and Stidsvig, Sweden, *Bull. Geol. Soc. Finland*, 58, 307-333 (1986).
24. Voight, B. and St. Pierre, B. H. P., Stress history and rock stress, Proc. 3rd Cong. Internat. Soc. for Rock Mechanics, Denver, CO., 580-582, (1974).
25. Zoback, M. D., Healy, J. H., Roller, J. C., Gohn, G. S. and Higgins, B. B., Normal faulting and in situ stress in the South Carolina coastal plain near Charleston, *Geology*, 6, 147-152 (1978).